Article

Reinforced HNA Backbone Hydration in the Crystal Structure of a Decameric HNA/RNA Hybrid

Timm Maier, Ingo Przylas, Norbert Strater, Piet Herdewijn, and Wolfram Saenger

J. Am. Chem. Soc., **2005**, 127 (9), 2937-2943• DOI: 10.1021/ja045843v • Publication Date (Web): 09 February 2005

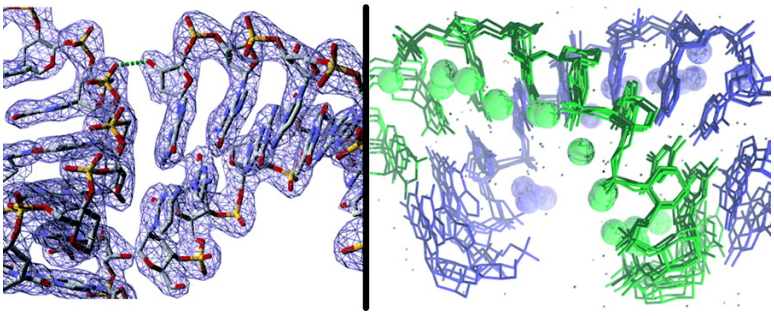

J|A|C|S
ARTICLES
Published on Web 02/09/2005

Reinforced HNA Backbone Hydration in the Crystal Structure of a Decameric HNA/RNA Hybrid

Timm Maier,[†,§] Ingo Przylas,[†] Norbert Strater,[†,¶] Piet Herdewijn,[‡] and Wolfram Saenger*[,†]

Contribution from the Institut für Chemie der Freien Universität Berlin, Takustrasse 6, 14195 Berlin, Germany, and Laboratory of Medicinal Chemistry, Rega Institute for Medical Research, Katholieke Universiteit Leuven, Minderbroedersstraat 10, B-3000, Leuven, Belgium

Received July 11, 2004; E-mail: saenger@chemie.fu-berlin.de

Abstract: The crystal structure of a decameric HNA/RNA (HNA = 2′,3′-dideoxy-1′,5′-anhydro-D-arabinohexitol nucleic acid) hybrid with the RNA sequence 5′-GGCAUUACGG-3′ is the first crystal structure of a hybrid duplex between a naturally occurring nucleic acid and a strand, which is fully modified to contain a six-membered ring instead of ribose. The presence of four duplex helices in the asymmetric unit allows for a detailed discussion of hydration, which revealed a tighter spinelike backbone hydration for the HNA- than for the RNA-strands. The reinforced backbone hydration is suggested to contribute significantly to the exceptional stability of HNA-containing duplexes and might be one of the causes for the evolutionary preference for ribose-derived nucleic acids.

Introduction

The base pairing between complementary strands of DNA and/or RNA is a key step in major information transfer processes of life, such as replication, transcription, and translation. In recent years, both biochemical research and medicine have begun to utilize the high specificity of duplex formation between complementary nucleic acid strands not only for the in vitro amplification of nucleic acids but also for turning off the expression of single genes in cells and tissues.[1−3] This approach, known as antisense technology, opened up new perspectives in the therapy of inherited diseases, cancer, and viral infections and has already given numerous insights into cellular regulation. Improvements to antisense technology have been made regarding both the delivery of antisense constructs to their cellular place of action in single cells, tissues, and complete organisms and the physicochemical properties of the antisense agents themselves. Modifications of nucleic acid backbone structure have led to an increased resistance to cellular nucleases, an improved solubility, and enhanced hybridization properties.[4−7]

One of the groups of promising antisense oligonucleotides currently being evaluated is the hexitol nucleic acids (HNA) composed of 2′,3′-dideoxy-1′,5′-anhydro-D-arabinohexitol nucleosides with 4′-6′-phosphodiester internucleotide linkages and with the base attached in axial position to the 2′-position (Figure 1a). HNA oligonucleotides have been tested as antimalarial agents and have also been targeted against *Ha-Ras*- and other mRNAs.[8,9] The replacement of the conformationally flexible deoxyribose by the restricted anhydrohexitol ring results in a structural preorganization of HNA to form A-type helices with efficient base stacking.[5] HNA is able to form Watson−Crick base-pair-mediated duplexes and hybrids with HNA, RNA, and DNA, with stability decreasing in the given order due to the conformational preferences of HNA for A-type helices. This also results in a strong preference of HNA for RNA over DNA in duplex formation. HNA/HNA and HNA/RNA duplexes are thermodynamically more stable than all naturally occurring nucleic acid double strands, making HNA a promising candidate for antisense applications.[10]

In contrast to DNA/RNA duplexes, the corresponding HNA/RNA hybrids are poorly hydrolyzed by RNAseH.[11,12] However, some nucleotide polymerizing enzymes accept anhydrohexitol nucleotides as substrates.[13] Mutants of HIV-1 reverse transcriptase are capable of elongating DNA primers with HNA nucleotides, performing a template-based enzymatic synthesis

† Institut für Chemie der Freien Universität Berlin.
‡ Katholieke Universiteit Leuven.
§ Present address: Institute for Molecular Biology and Biophysics, Hönggerberg HPK building, ETH Zürich, CH-8093 Switzerland.
¶ Present address: Biomedizinisches und Biotechnologisches Zentrum der Universität Leipzig, Johannisallee 29, 04103 Leipzig, Germany.

(1) Lebedeva, I.; Stein, C. A. *Annu. Rev. Pharmacol. Toxicol.* **2001**, *41*, 403−419.
(2) Crooke, S. T. *Methods Enzymol.* **2000**, *313*, 3−45.
(3) Yuen, A. R.; Sikic, B. I. *Front. Biosci.* **2000**, *5*, D588−D593.
(4) Akhtar, S.; Hughes, M. D.; Khan, A.; Bibby, M.; Hussain, M.; Nawaz, Q.; Double, J.; Sayyed, P. *Adv. Drug Delivery Rev.* **2000**, *44* (1), 3−21.
(5) Herdewijn, P. *Biochim. Biophys. Acta* **1999**, *1489* (1), 167−179.
(6) Herdewijn, P. *Antisense Nucleic Acid Drug Dev.* **2000**, *10* (4), 297−310.
(7) Larsen, H. J.; Bentin, T.; Nielsen, P. E. *Biochim. Biophys. Acta* **1999**, *1489* (1), 159−166.
(8) Vandermeeren, M.; Preveral, S.; Janssens, S.; Geysen, J.; Saison-Behmoaras, E.; Van Aerschot, A.; Herdewijn, P. *Biochem. Pharmacol.* **2000**, *59* (6), 655−663.
(9) Flores, M. V.; Atkins, D.; Stewart, T. S.; Van Aerschot, A.; Herdewijn, P. *Parasitol. Res.* **1999**, *85* (10), 864−866.
(10) Van Aerschot, A.; Verheggen, I.; Hendrix, C.; Herdewijn, P. *Angew. Chem., Int. Ed.* **1995**, *34* (12), 1338−1339.
(11) Hendrix, C.; Rosemeyer, H.; De Bouvere, B.; Van Aerschot, A.; Seela, A.; Herdewijn, P. *Chem.—Eur. J.* **1997**, *3*, 1513−1520.
(12) Zamaratski, E.; Pradeepkumar, P. I.; Chattopadhyaya, J. *J. Biochem. Biophys. Methods* **2001**, *48* (3), 189−208.
(13) Vastmans, K.; Pochet, S.; Peys, A.; Kerremans, L.; Van Aerschot, A.; Hendrix, C.; Marliere, P.; Herdewijn, P. *Biochemistry* **2000**, *39* (42), 12757−12765.

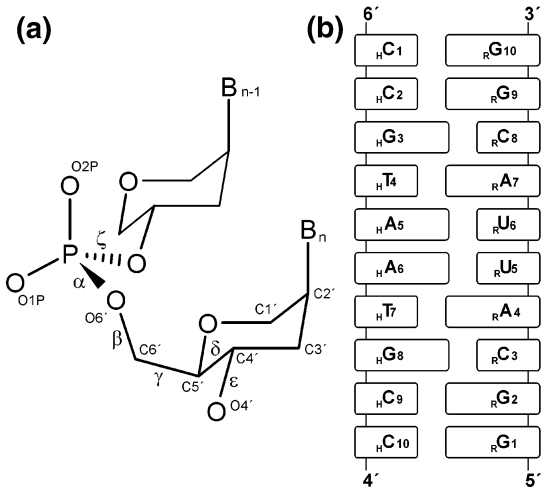

Figure 1. Chemical structure of HNA/RNA. (a) General chemical structure, numbering, and torsion angle definition of HNA oligonucleotides, and (b) base numbering and base pairs in the crystallized HNA/RNA decamer.

of HNA oligonucleotides.[14] HNA itself may serve as a template for the chemical synthesis of DNA or RNA.[15] Though the natural occurrence of HNA in evolution is unlikely, it can serve as a model system for nucleic acid derivatives with six-membered conformationally rigid carbohydrate rings that are capable of storing and transferring evolutionary information and are treated in ongoing discussions on the etiology of nucleic acids.[16−19]

HNA/RNA hybrids form A-type helices in solution, as shown by high-resolution NMR and CD spectrometry of an octameric HNA/RNA hybrid and in agreement with molecular dynamics simulations. The well-defined NMR structure suggested a reduced conformational flexibility and a rigid conformation of HNA/RNA hybrids.[20−22] In contrast, crystal structures of double-helical HNA oligomers indicated a certain extent of structural flexibility.[23] To further analyze the structural constraints on HNA/RNA hybrids and their hydration properties, we have determined the X-ray crystal structure of a decameric HNA/RNA hybrid to 2.6 Å resolution.

Methods

Synthesis, Purification, and Crystallization. The decameric ribo-oligonucleotides, 5′-GGCAUUACGG-3′, and brominated 5′-GGCA-(5-Br-rU)UACG were purchased from TIB MOLBIOL (Berlin, Germany) and CyberSyn (Lenni, PA), respectively. The complementary decameric HNA was synthesized using a phosphoramidite approach as described.[22] Purification of single-stranded oligomers was achieved by ion-exchange chromatography on a Mono Q 5/5 column (Pharmacia, Uppsala, Sweden) under denaturing conditions. Oligomers were applied in 10 mM NaOH and eluted with a linear gradient of 0−1 M NaCl in 10 mM NaOH at a flow rate of 1 mL/min. For hybridization, HNA and RNA strands were desalted on Sephadex G10, dissolved in 10 mM Tris, pH 8.0, and mixed in equal molar concentrations as judged by UV absorption. The resulting hybrid duplex was purified by ion-exchange chromatography on a Mono Q column under native conditions in a gradient of 0−1 M NaCl in 10 mM Tris/HCl, pH 8.0. The purified hybrid duplexes were buffer exchanged on Sephadex G10 to 10 mM Tris/HCl, pH 8.0, and concentrated to yield a 1 mM solution. For crystallization trials, the hanging-drop vapor diffusion method was used, with drops consisting of 2 μL of hybrid solution and 2 μL of reservoir equilibrated against 800 μL of reservoir solution. The final reservoir solutions for crystal growth were 0.9 M Li_2SO_4, 10 mM $Mg(CH_3COO)_2$, and 100 mM Tris/HCl, pH 8.0, and 1.4 M Li_2SO_4, 10 mM $Mg(CH_3COO)_2$, and 100 mM Tris/HCl, pH 8.0, for the native and single-site-brominated HNA/RNA duplexes, respectively. Crystals appeared only after six months.

Table 1. Data Collection and Refinement Statistics

	λ1	λ2	λ3	native
space group	$P4_12_12$	$P4_12_12$	$P4_12_12$	$P4_12_12$
cell parameters *a*,*c* (Å)	114.8, 54.8	114.8, 54.8	114.8, 54.8	113.8, 55.4
temperature (K)	100	100	100	100
wavelength (Å)	0.90898	0.92018	0.92086	0.92067
mosaicity (deg)	0.35	0.35	0.36	0.63
reflections	189890	189899	189958	193723
unique reflections	21510	21506	21507	11676
resolution (Å)	35−2.6	35−2.6	35−2.6	35−2.6
R_{sym} (%)	5.6	5.2	5.3	6.0
completeness (%)	99.9	99.9	99.9	99.4
I/sigma[a]	27.0 (3.0)	29.2 (3.3)	29.0 (3.2)	28.7 (3.2)
Wilson *B* factor (Å^2)	76.9	77.3	77.7	76.3
	native			
reflections, cutoff	11667, none			
R, R_{free} (%)	21.7, 25.4			
rmsd bonds (Å)	0.008			
rmsd angles (deg)	1.25			
rmsd dihedrals (deg)	10.40			
rmsd impropers (deg)	1.38			
No. of nucleic acid base pairs/atoms	40/1688			
No. of water molecules	166			
No. of sulfate ions/atoms	5/25			
solvent content (%)	66.2			
average *B* nucleic acid (Å^2)	47.7			
average *B* water (Å^2)	45.2			

[a] Statistics of data collection and refinement; values for the highest resolution shell (2.60−2.69 Å) are given in parentheses.

Data Collection. For cryogenic X-ray data collection, crystals were transferred to Paratone-N (Exxon Chemical Co.), and the mother liquor was stripped off by moving the crystal in the oil. Subsequently, the crystal was mounted in a loop and flash-frozen at 100 K in a stream of nitrogen gas. Multiwavelength anomalous diffraction (MAD) data of a crystal of HNA/Br−RNA as well as diffraction data on native HNA/RNA were collected on a MAR345 Image Plate at BM30 (ESRF, Grenoble, France). Data collection statistics are given in Table 1.

Structure Determination and Refinement. Crystallographic data were processed with the HKL program suite.[24] The phase problem was initially solved by MAD using 2.6 Å resolution data for a single-site-brominated HNA/5-Br−uridine−RNA crystal. Phases were improved with the programs MLPHARE and DM.[25] A model was built with O[26] based on an initial A-helical geometry generated using XPLOR.[27]

(14) Vastmans, K.; Froeyen, M.; Kerremans, L.; Pochet, S.; Herdewijn, P. *Nucleic Acids Res.* **2001**, *29* (15), 3154−3163.
(15) Kozlov, I. A.; Politis, P. K.; Van Aerschot, A.; Busson, R.; Herdewijn, P.; Orgel, L. E. *J. Am. Chem. Soc.* **1999**, *121* (12), 2653−2656.
(16) Schoning, K.; Scholz, P.; Guntha, S.; Wu, X.; Krishnamurthy, R.; Eschenmoser, A. *Science* **2000**, *290* (5495), 1347−1351.
(17) Eschenmoser, A. *Science* **1999**, *284* (5423), 2118−2124.
(18) Beier, M.; Reck, F.; Wagner, T.; Krishnamurthy, R.; Eschenmoser, A. *Science* **1999**, *283* (5402), 699−703.
(19) Lescrinier, E.; Froeyen, M.; Herdewijn, P. *Nucleic Acids Res.* **2003**, *31* (12), 2975−2989.
(20) Hendrix, C.; Rosemeyer, H.; Verheggen, I.; Seela, A.; Van Aerschot, A.; Herdewijn, P. *Chem.−Eur. J.* **1997**, *3* (1), 104−114.
(21) Lescrinier, E.; Esnouf, R.; Schraml, J.; Busson, R.; Heus, H.; Hilbers, C.; Herdewijn, P. *Chem. Biol.* **2000**, *7* (9), 719−731.
(22) De Winter, H.; Lescrinier, E.; Van Aerschot, A.; Herdewijn, P. *J. Am. Chem. Soc.* **1998**, *120* (22), 5381−5394.
(23) De Clercq, R.; Van Aerschot, A.; Read, R. J.; Herdewijn, P.; Van Meervelt, L. *J. Am. Chem. Soc.* **2002**, *124* (6), 928−933.
(24) Otwinowski, Z.; Minor, W. *Methods Enzymol.* **1997**, *276*, 307−326.
(25) CCP4; *Acta Crystallogr., Sect. D* **1994**, *50*, 760−763.
(26) Jones, T. A. *J. Appl. Crystallogr.* **1987**, *11*, 268−272.
(27) Brunger, A. T. *X-PLOR*, version 3.1; Yale University Press: New Haven and London, 1992.

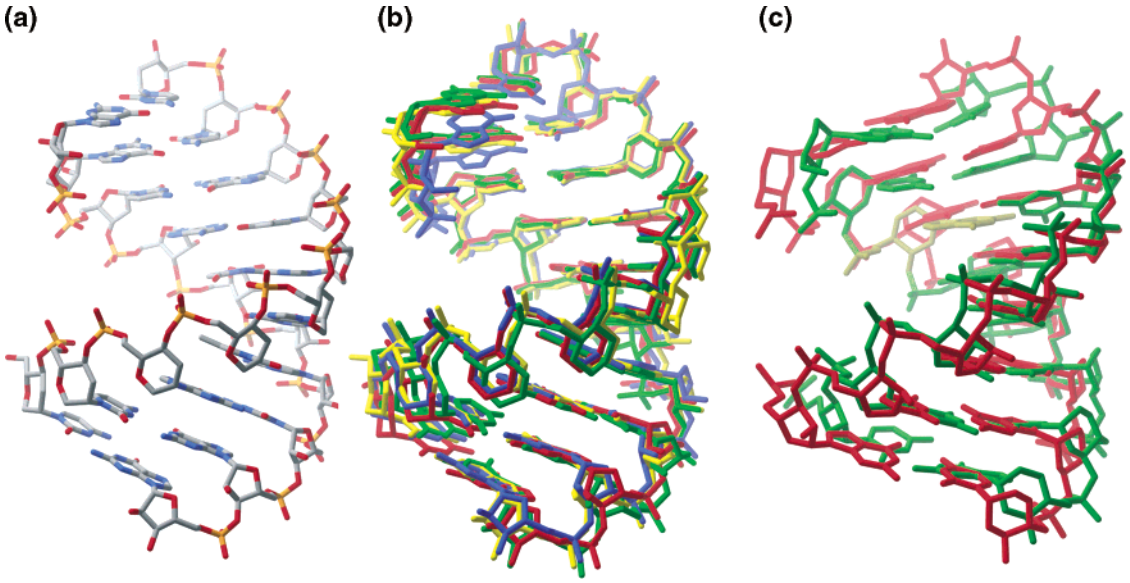

Figure 2. Structural overview and comparison to NMR solution structure. (a) Duplex D1 colored by atom type; (b) superimposition of D1 (yellow), D2 (blue), D3 (green), and D4 (red); (c) superimposition of the NMR solution structure of the octameric HNA/RNA duplex, h(3′GCGATGCG5′) r(5′CGCUACGC3′) [PDB ID 1EJZ] (green), by least-squares fitting of the backbone atoms defining the torsion angles, $\alpha - \zeta$, for the central six base pairs to the corresponding atoms of the decameric HNA/RNA duplex D1 described here (red); the rmsd obtained for this fit is 2.7 Å.

This model was used for refinement with CNS[28] against the isomorphous native HNA/RNA data. Parameters for HNA were adapted from A-DNA/RNA and an HNA mononucleotide X-ray structure.[29,30] Torsional restraints for HNA were scaled down during refinement. Refinement statistics are given in Table 1. Helical parameters were analyzed with the programs RNA[31] and CURVES[32] in accordance with EMBO nomenclature.

Coordinates. The coordinates and reflection data for the HNA/RNA decamer have been deposited in the Macromolecular Structure Database under accession code pdb: 26J6.

Results and Discussion

Overall Molecular Structure of the HNA/RNA Hybrid. The crystallographic asymmetric unit contains four hybrid duplexes termed D1−D4 in the order of increasing maximum *B* values. The individual hybrid duplex helices are stabilized by standard Watson−Crick base pairs. The nucleotides are termed $_{H}$C1−$_{H}$C10 in 6′ → 4′ direction on the HNA strand and $_{R}$G1−$_{R}$G10 in 5′ → 3′ direction on the complementary RNA strand, that is, $_{H}$C1 is paired to $_{R}$G10 (Figure 1b). All of the RNA strand ribose rings are in C3′-endo conformation typical of A-RNA duplexes, and the HNA strand anhydrohexitol rings are in a chair conformation, equivalent to $^{4}C_{1}$ in hexoses.

D1−D4 differ from each other in their temperature factors and local geometric parameters (see below) but share common overall structural features (Figure 2a,b and Table 2). The helical rise for all duplexes is between 2.5 and 2.6 Å, and the helical twist ranges from 30.8 to 32.7°, in good agreement with an A-type helical geometry[33] (Table 2). This helical class is also indicated by the displacement of base pairs in *x*-direction relative to the helical axis (X_{disp}) ranging from −5.0 to −5.4 Å compared to −5.2 Å for A-RNA and −0.6 Å for B-DNA. Helix D2 obeys a standard A-type geometry with helical twist of 32.7°. In contrast, the reduced helical twists of 30.8, 31.1, and 31.3° for D1, D3, and D4, respectively, as well as a base pair inclination lower than that of a standard A-RNA structure, classify these three duplexes as the A′-subtype helical conformation, with 12 rather than 11 base pairs per helical turn (see Table 2).[34,35]

The structural differences between D2 and D1, D3, and D4 are evidenced by RMS deviations of atom positions for the least

Table 2. Classification of Mean Helical Parameters for the Individual Duplexes[a]

molecule	X_{disp} (Å)	inclination (deg)	twist (deg)	rise (Å)	minor groove width (Å)[b]
D1	-5.4 ± 1.4	13.2 ± 5.9	30.8 ± 3.5	2.6 ± 0.3	9.9 ± 0.4
D2	-5.4 ± 1.7	16.3 ± 6.5	32.7 ± 6.2	2.5 ± 0.4	10.0 ± 0.3
D3	-5.3 ± 1.6	14.6 ± 5.4	31.1 ± 3.6	2.6 ± 0.3	10.3 ± 0.5
D4	-5.0 ± 0.8	11.9 ± 8.6	31.3 ± 4.0	2.6 ± 0.4	10.0 ± 0.3
AR0005[c]	-4.7	12.1	30.4	2.9	9.8
AH0001[c]	-5.2	10.5	30.9	3.0	9.8
NMR[d]	-3.4		34.4	3.0	10.0
NMR[e]	-2.6	10.3	36.4	2.8	
A-RNA[f]	-5.2	16.1	32.7	2.8	10.9
A′-RNA[f]	-5.3	10.3	30.0	3.0	10.8
B-DNA[f]	-0.6	-4.6	36.0	3.4	5.5

[a] Helical parameters were calculated with the program RNA (ref 28). [b] Minor groove width is measured as the closest interstrand P−P distances subtracted by 5.8 Å to account for the van der Waals radii of the phosphate groups. [c] Data for the A′-helical tridecameric RNA duplex (AR0005) and the decameric DNA/RNA hybrid (AH0001) were taken from the original publications (refs 34 and 35). [d] Data for the NMR solution structure of an octameric HNA/RNA duplex were taken from the original publication, calculated with the CURVES program, ignoring one terminal base pair. [e] Data for the NMR solution structure of an octameric HNA/RNA duplex were taken from the original publication, calculated for the complete duplex by the RNA program. [f] Values for the average structures of A-RNA, A′-RNA, and B-DNA from fiber diffraction are cited from ref 35.

(28) Brunger, A. T.; Adams, P. D.; Clore, G. M.; DeLano, W. L.; Gros, P.; Grosse-Kunstleve, R. W.; Jiang, J. S.; Kuszewski, J.; Nilges, M.; Pannu, N. S.; Read, R. J.; Rice, L. M.; Simonson, T.; Warren, G. L. *Acta Crystallogr., Sect. D* **1998**, *54*, (5), 905−921.
(29) De Clercq, R.; Herdewijn, P.; Van Meervelt, L. *Acta Crystallogr., Sect. C* **1996**, *52*, 1213−1215.
(30) De Clercq, R.; Van Aerschot, A.; Herdewijn, P.; Van Meervelt, L. *Acta Crystallogr., Sect. D* **1999**, *55*, (1), 279−280.
(31) Babcock, M. S.; Pednault, E. P.; Olson, W. K. *J. Mol. Biol.* **1994**, *237* (1), 125−156.
(32) Lavery, R.; Sklenar, H. *J. Biomol. Struct. Dyn.* **1989**, *6* (4), 655−667.
(33) Saenger, W. *Principles of Nucleic Acid Structure*; Springer-Verlag: Berlin, Heidelberg, New York, 1988.
(34) Conn, G. L.; Brown, T.; Leonard, G. A. *Nucleic Acids Res.* **1999**, *27* (2), 555−561.
(35) Tanaka, Y.; Fujii, S.; Hiroaki, H.; Sakata, T.; Tanaka, T.; Uesugi, S.; Tomita, K.; Kyogoku, Y. *Nucleic Acids Res.* **1999**, *27* (4), 949−955.

squares superposition of all four duplexes that are larger for the superpositions of D1, D3, or D4 on D2 than for all other superpositions (see Supporting Information Table S1). Five sulfate ions were identified in the electron density map. Four of them are bound on the major groove sides of base pairs and interact mainly with amino groups of cytosine and adenine. Two out of these four sulfates are bound to the terminal residues of two distinct helices, and the other two are bound closer to the middle of the helices. The fifth sulfate is bound on the minor groove side close to $_{R}$G1 at the terminus of D3 and interacts only with the RNA strand, forming weak hydrogen bonds not only with base atoms but also with hydroxyl groups of the ribose moieties.

Influence of Crystal Packing on *B* Values and Local Conformation. Only very few crystal structures of full-length RNA/DNA hybrids have been determined, and none of them contains more than two duplexes per asymmetric unit. By contrast, the asymmetric unit of HNA/RNA crystals described here contains four individual duplexes (Figure 3a). The large number of 80 nucleotides per asymmetric unit allows for a verification of helical geometry and hydration properties, independent of specific packing interactions. It also provides the possibility to analyze the conformational flexibility or rigidity of the hybrid duplex. The overall differences between all four molecules are small, with an average rmsd of 1.2 ± 0.2 Å, and the deviation between the duplexes increases toward the terminal base pairs (Figure 2b). Nevertheless, pronounced differences in local conformation are observed.

In duplexes D2 and D3, one RNA nucleotide each exhibits an alternative backbone conformation compared to all other residues; the α and γ backbone torsion angles between $_{R}$A7 and $_{R}$C8 in D2 and between $_{R}$U5 and $_{R}$U6 in D3 are in a (*t*,*t*)- instead of the usual (*g*−,*g*+)-conformation (see Supporting Information Figure S2). Such alterations have previously been observed in RNA/DNA hybrid duplexes and in A-DNA and A-RNA helices.[36] In contrast to these cases, the unusual backbone conformation of one strand in HNA/RNA is not compensated by a similar alteration in the complementary strand. As a direct consequence of the (*t*,*t*)-conformation, the O5′ atom lies on the minor instead of the major groove side of the helix.[34] The four nucleotides showing local deformation are part of crystal contact sites between the minor grooves of two HNA/RNA helices (see below) and permit the formation of optimal hydrophobic contacts between adjacent molecules in the crystal. The altered backbone torsion angles, α and γ, are less important for the overall helical structure and do not correlate significantly with base-step parameters.[37] Similar, but smaller deviations at a crystal contact site are found between residues $_{H}$A5 and $_{H}$A6 of D4. Here, mainly the β, ϵ, and ζ torsion angles deviate from the mean by approximately 40°, leading to a decreased $\epsilon - \zeta$ value and an increased shift of the corresponding base pair (see Supporting Information Figure S2).

The helical twist and the roll-slide-twist group of base-step parameters are strongly correlated between all four molecules, though the patterns of crystal contacts (see below) and the local structural deviations are not (see Supporting Information Figure S3). Thus, the deviations in these parameters are indicators for sequence-specific differences in the conformations of the HNA/RNA duplexes, as commonly observed in nonmodified nucleic acid helical structures.[37,38]

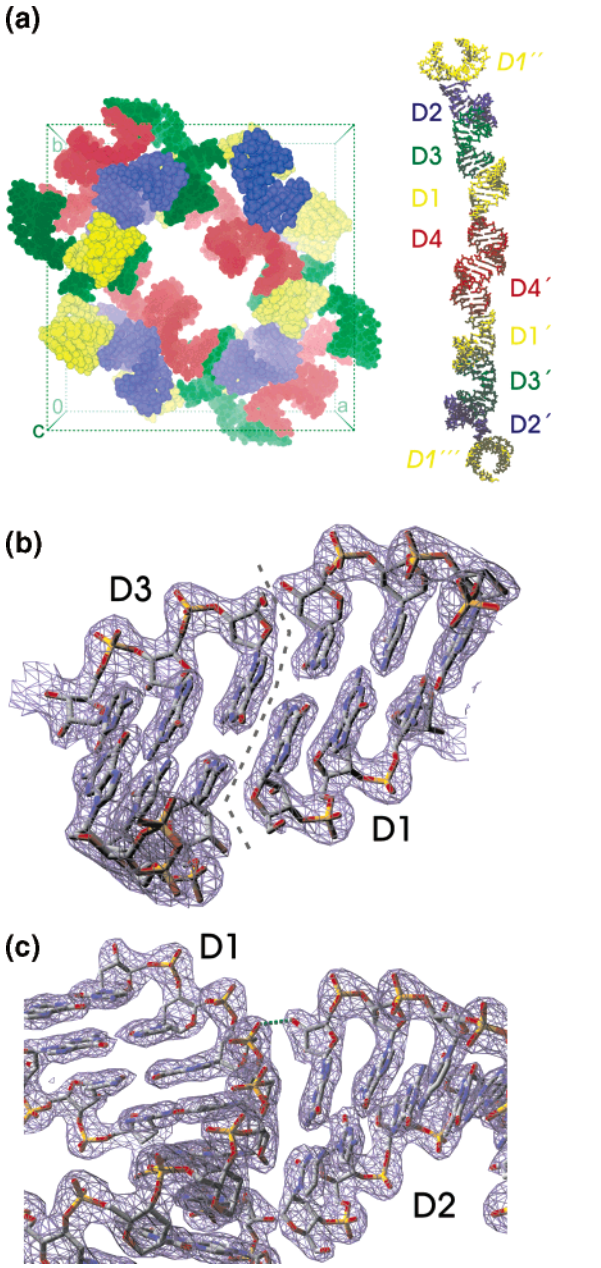

Figure 3. Crystal packing of HNA/RNA. (a) The individual duplexes (left) in one unit cell are shown as CPK models. Large solvent channels extend parallel to the *c*-axis. The solvent-exposed regions of D4 (red) lining the solvent channel at *x*,*y* = 0.5 have the largest temperature factors of all molecules. (Right) Pseudocontinuous superhelix extending over multiple unit cells; color coding is the same as in Figure 2b. (b) Pseudocontinuous stacking of D1 and D3, separated by a dashed line. (c) Contact in which D2 protrudes toward the minor groove of D1; the hydrogen bond between the terminal O3′ of $_{R}$G10 (D2) and O1P of $_{H}$G8 is indicated by a dashed line. In (b) and (c), molecules are shown as stick models together with a (2Fo−Fc) electron density map contoured at 1.3 sigma.

Different packing modes have been observed in oligonucleotide crystals. In crystals of B-DNA, end-to-end stacking produces continuous helices, and interactions occur between the minor grooves as well as between the major grooves.[36] A-DNA helices always stack with their terminal base pairs against the

(36) Horton, N. C.; Finzel, B. C. *J. Mol. Biol.* **1996**, *264* (3), 521−533.
(37) Packer, M. J.; Hunter, C. A. *J. Mol. Biol.* **1998**, *280* (3), 407−420.
(38) Packer, M. J.; Dauncey, M. P.; Hunter, C. A. *J. Mol. Biol.* **2000**, *295* (1), 85−103.

wide and shallow minor groove of neighboring duplexes.[39] In A-RNA crystals, helices are often packed pseudocontinuous by an end-to-end stacking with such a low helical twist that these helices cannot be considered continuous, and hydrogen bonds between the 2′-OH groups of neighboring duplexes stabilize the crystal packing. Crystals of DNA/RNA hybrids may exhibit features from several of these packing modes, such as end-to-end stacking to form pseudocontinuous helices, insertion of the end of one duplex in the minor groove of another helix, as well as unique solvent-mediated interactions between the minor grooves.[36]

In HNA/RNA, extensive crystal contacts are formed between the individual molecules. The crystal is built up from pseudocontinuous superhelices containing eight molecules in the order D2, D3, D1, D4, D4, D1, D3, D2. The superhelices start and end with D2 protruding toward the minor grooves of D1 molecules in neighboring unit cells.

The D2/D3, D3/D1, and D1/D4 stacks are in head-to-tail direction (Figure 3b), but D4 is stacked head-to-head to a symmetry related D4. While D3/D1 stacks are oriented HNA on RNA and RNA on HNA, leading to G−C on top of C−G base pairs, D2/D3 stacks are packed HNA on HNA and RNA on RNA (G−C on G−C). The helical twist for the superhelical connections of two helices is for all helix stacks unusually nonpositive. For D1/D4 and D2/D3, the helical twists are approximately −40°; for D1/D3, it is −15°, and it is only −5° for the connection of two symmetry related copies of D4.[36] The helical rise over all superhelix stacks is between 2.5 and 3.3 Å, very similar to the intrahelical rise. The interaction between D2 and D1 at the ends of the superhelices is primarily stabilized by hydrophobic contacts between the hexitol rings of $_{H}$A6 and $_{H}$T7 of D1 with the parallel positioned $_{R}$G10/$_{H}$C1 base pair of D2. Only one strong interduplex hydrogen bond connects D2 and D1, formed between the terminal O3′ H of $_{R}$G10 (D2) and O1P of $_{H}$G8 (D1) (Figure 3c), in contrast to similar contacts, which are mediated by a larger number of hydrogen bonds.[36]

Besides being part of these unusual noninfinite superhelices, all duplexes form contacts with both of their strands to one or two of the other molecules. These interactions are formed between the minor grooves of two helices in different ways; the contact between D1 and D2 is stabilized by direct hydrogen bonds between the O2′-hydroxyl group of the $_{R}$G2, $_{R}$C3, and $_{R}$A4 (D2) residues and the O or N atom in the minor groove of HNA and RNA strands (D1). The hexitol rings of $_{H}$C9 (D2) and $_{H}$G3 (D1), as well as the ribose of $_{R}$A4 (D2) and the hexitol group of $_{H}$T4 (D1), are orientated in parallel and interact in a hydrophobic manner. Water molecules are excluded from the interface area between D1 and D2, except for two waters that mediate indirect hydrogen bonds between the two duplexes. In a very similar manner, the contact between D2 and D4 is formed by direct hydrogen bonds involving O2′-H of ribose moieties, indirect water-mediated hydrogen bonds, and hydrophobic contacts. Water-mediated hydrogen bonds are also formed between residues of D1 and D3, which are in further direct contact only by hydrophobic interactions.

The distribution of temperature factors shows significant variations between the four molecules (see Supporting Information Figure S4). The average temperature factors per residue range from 24 to 75 Å^2, where *B* values are largest for the phosphate groups, lowest for the bases, and intermediate for the sugars. Only D1 displays a constantly low-temperature factor of around 30 Å^2 for all residues, probably because it forms a large number of intermolecular contacts to all other duplexes. For D2−D4, the temperature factors are generally greater in regions without contacts to other duplexes. In some base pairs, even the *B* values for the respective HNA and RNA residue differ by more than 15 Å^2, where contacts are formed by one of the residues only (e.g., $_{H}$T7−$_{R}$A4 in D2; $_{H}$A6−$_{R}$U5 in D4). *B* values also correlate between contacting residues from different molecules.

Table 3. Distribution of Hydrating Water Binding Sites[a]

	HNA/RNA		dsHNA-tri[c]		A-RNA		A-DNA	
	total	relative	total	relative	total	relative	total	relative
phosphates	76	0.35	19	0.40	51	0.31	57	0.52
sugars[b]	57	0.26	13	0.28	64	0.37	10	0.09
bases	86	0.39	15	0.32	55	0.32	43	0.39
No. of base pairs	40		8		8		8	

[a] Total and relative numbers of hydrogen bonds to phosphates, sugars, and bases in HNA/RNA (this work) and in high-resolution crystal structures of A-RNA and A-DNA[41] are given. [b] The differences in sugar hydration between RNA and DNA are due to the presence or absence of the O2′ atom. HNA 2′,3′-dideoxy-1′,5′-anhydro-D-arabinohexitols have a relative number of hydrogen bonds to water molecules higher than that of DNA deoxyriboses because they participate with their O6′ atom in the backbone hydrating water network. [c] For dsHNA, only the higher resolution trigonal crystal form is analyzed, where the asymmetric unit contains only one strand of the duplex; the second one is generated by crystallographic symmetry.[23]

Hydration. The hydration of nucleic acids is considered a major factor determining duplex stability and thermodynamics of duplex formation even in the case of conformationally restricted oligonucleotides[5,22] and is of great interest in the search for potent antisense drugs.[40] However, hydration of HNA oligonucleotides has not been experimentally analyzed so far. Despite a resolution of only 2.6 Å and the partially high-temperature factors, a total of 166 hydrating waters could be located reliably in the HNA/RNA crystal structure. The distribution of hydrogen bonds between water molecules and bases, sugars, and phosphates is similar to those reported for high-resolution structures of oligonucleotides, indicating a correct assignment of water molecules.[41] It is also consistent with the hydration pattern of a dsHNA oligonucleotide[23] (Table 3).

The hydration of bases is very similar between the HNA and RNA strands. Preferred base hydration sites are N4 of cytidine, O6 of Guanine, and N6 of adenine, all located in the major groove. A similar hydration pattern for bases has been observed in high-resolution structures of A-DNA and A-RNA.[42,43] A quantitative analysis of base hydration is not possible due to the large differences in *B* values for equivalent bases and to the nonconserved positions of crystal contacts.

Backbone hydration plays an important role for nucleic acid conformation and stability.[40,44] Unfortunately, different nomenclatures for free, nonesterified phosphate oxygens are in common

(39) Wahl, M. C.; Sundaralingam, M. *Biopolymers* **1997**, *44* (1), 45−63.
(40) Egli, M.; Tereshko, V.; Teplova, M.; Minasov, G.; Joachimiak, A.; Sanishvili, R.; Weeks, C. M.; Miller, R.; Maier, M. A.; An, H.; Cook, P. D.; Manoharan, M. *Biopolymers* **1998**, *48* (4), 234−252.
(41) Egli, M.; Portmann, S.; Usman, N. *Biochemistry* **1996**, *35* (26), 8489−8494.
(42) Klosterman, P. S.; Shah, S. A.; Steitz, T. A. *Biochemistry* **1999**, *38* (45), 14784−14792.
(43) Auffinger, P.; Westhof, E. *J. Biomol. Struct. Dyn.* **1998**, *16* (3), 693−707.
(44) Saenger, W.; Hunter, W. N.; Kennard, O. *Nature* **1986**, *324* (6095), 385−388.

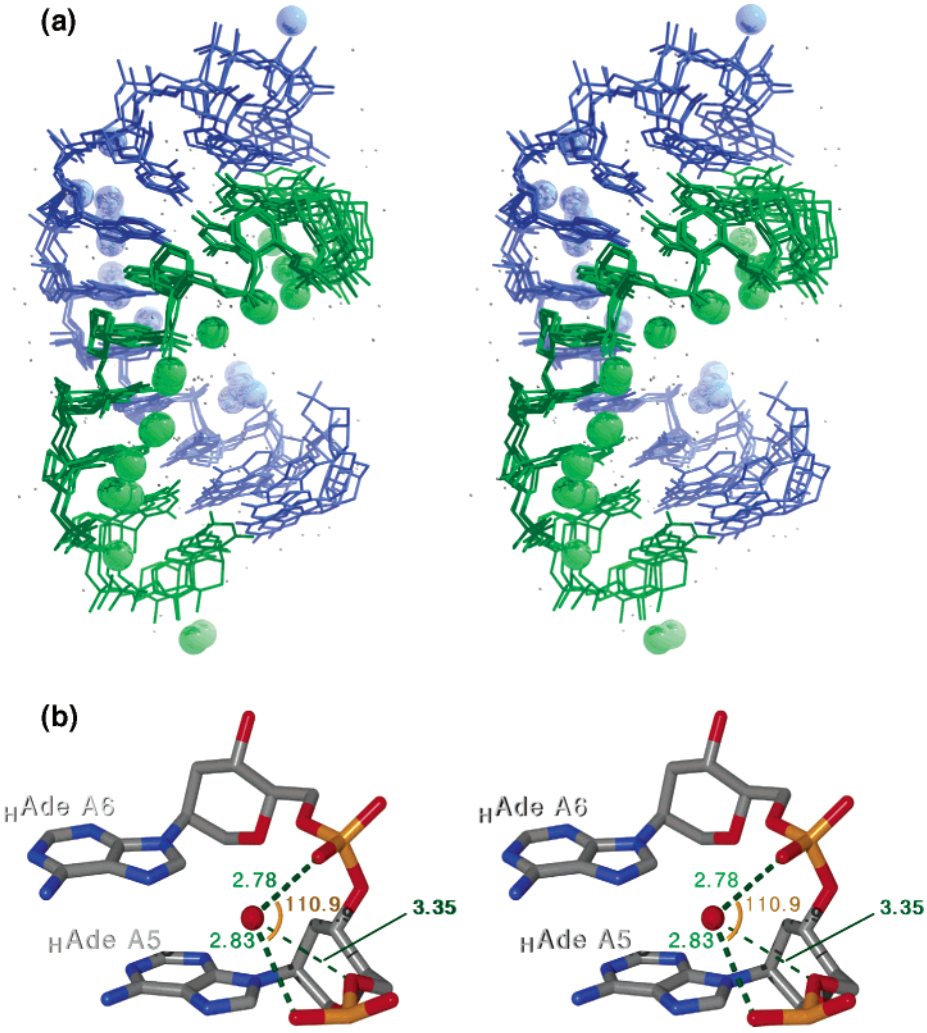

Figure 4. Backbone hydration of HNA/RNA (stereo). (a) The HNA and RNA strands of D1−D4 are superimposed and shown in green and blue, respectively. Waters involved in spinelike backbone hydration bridging adjacent O2P atoms are shown as large balls in identical colors. All other water molecules are shown as small blue dots. The positions of water molecules involved in phosphate bridging are much better conserved in HNA than in RNA. Only in HNA, but not in RNA, bridging waters could be identified for all base-pair steps. (b) Geometry of bridging water binding for a selected base step. Hydrogen bond distances (Å) and opening angle (deg) are indicated. The conservation of this geometry is obvious from (a), though distances may vary slightly between the individual base steps due to local disturbances introduced by crystal contacts.

Table 4. Distribution of Hydrating Water Binding Sites of Backbone Oxygen Atoms

	HNA strand	RNA strand	dsHNA-tri[b]	dsHNA-hex[c]	A-RNA
O1P	1.0	1.0	1.0	1.0	1.0
O2P	3.6	2.0	1.9	3.0	1.7
O6′/O5′	1.1	0.5	1.1	1.0	0.5
O4′/O3′	0.5	0.7	0.6	0.7	0.6
O2′		2.0			1.4

[a] Numbers of hydrogen bonds between hydrating waters and O1P, O2P, and O6′/ O5′ of the HNA/RNA strand of D1 to D4 (this work) compared to numbers obtained from crystal structures of A-RNA[41] and of dsHNA.[23] Numbers are given relative to the number of hydrogen bonds between hydrating waters and O1P atoms. [b] Trigonal crystal form in space group $P3_212$. [c] Hexagonal crystal form in space group $P6_222$

use. Here, we obey the recommendations of IUPAC[45] (Figure 1a), which vary with some of the cited publications. The hydration pattern of the backbone phosphate and nonring sugar oxygen atoms is very similar between the A-RNA and the RNA strand of HNA/RNA (Table 4). By contrast, the HNA strand has a backbone hydration pattern significantly different than that of the RNA strand in the same structure under the same conditions; O2P is about twice as strongly hydrated in the HNA than in the RNA strands (Figure 4a). In addition, the O6′ of the HNA strands shows an increased number of hydrating waters compared to the equivalent O5′ of RNA (Table 4). Because of the large number of different base pairs analyzed, these results cannot be biased by crystal packing. An analysis of the geometric properties of the HNA backbone provides an explanation for these differences in hydration. For a standard A-helical conformation, the expected P−P distance between two successive phosphorus atoms is 5.9 Å,[33] very close to the value observed for the RNA strands of D1−D4, 5.85 Å. For the HNA strands, a shortened P−P distance of only 5.55 Å is observed. These P−P distances are significantly different at the 95% significance level, according to an analysis of variances test (ANOVA), and allow for tighter water-mediated bridging of O2P atoms from adjacent backbone phosphates in the HNA compared to the RNA oligomer. The bridging water molecules are also at typical long hydrogen bonding distance to the O6′ of the hexitol groups, further reinforcing hydration (Figure 4b).

(45) IUPAC−IUB Joint Commission on Biochemical Nomenclature, Newsletter 1984. *Eur. J. Biochem.* **1984**, *138*, 5−7.

In the two reported hexagonal and trigonal crystal structures of dsHNA,[23] the average P−P distances are 5.5 and 5.7 Å, respectively, and comparable to those observed in HNA/RNA. This is associated with a comparable pattern of backbone hydration, although the crystal environments are completely different; the hydration of O2P is more pronounced in HNA (for both, dsHNA, and the HNA/RNA hybrid) than in dsRNA or the RNA strand in HNA/RNA, and in the HNA strands, a reinforced hydration of O6′ (termed O5′ in ref 23) is observed. The enhanced spinelike backbone hydration of HNA as compared to that of RNA has been associated with the extraordinary HNA duplex stability.[10]

Comparison with the Solution Structure of an HNA/RNA Duplex. The solution NMR structure of the octameric HNA/RNA duplex, h(3′-GCGATGCG-5′) r(5′-CGCUACGC-3′), has been described to be of the A-form,[21] consistent with CD spectroscopy.[19] The helical parameters indicate an average of A- and B-type structure (Table 2). This contrasts the X-ray crystal structure of the decameric HNA/RNA hybrid (Figure 1c). The main differences are the average helical twist, which is 3 to 5° lower in the X-ray structure, and the *X* displacement (X_{disp}) of −5 Å in the structure described here compared to −3.4 Å in the NMR solution structure. Both of these parameters are sensitive descriptors of the helix geometry. The minor groove width, however, is nearly identical for both structures. Although the sequences and lengths of the duplexes used in both studies are different, this probably does not cause the observed dissimilarities. A stronger influence may be expected from the different salt concentrations; the oligonucleotides are dissolved in pure D_2O or water for the NMR studies, while in the crystallization, 1.1−1.4 M lithium sulfate is used as precipitant.

Conclusions

We have determined the 2.6 Å resolution X-ray crystal structure of a decameric HNA/RNA duplex containing all four Watson−Crick base pairs and representing the physiologically active state of an HNA antisense oligonucleotide hybridized with target RNA. The asymmetric unit contains four distinct hybrid duplexes that differ only slightly in their overall helical conformation. Significant local structural disturbances could be attributed to crystal contacts. The crystal packing of HNA/RNA is one of the most complex arrangements that have been described for oligonucleotides; it includes pseudocontinuous superhelices of defined lengths, contacts of the terminal base pairs of one duplex with the minor groove of an adjacent one, and interactions between minor grooves of two duplexes.

The pronounced influence of crystal packing on the structure of the duplex, resulting in differences in helical twist of up to 2° and backbone torsion angle flips in RNA and even in HNA, demonstrates a higher degree of flexibility than expected for the conformationally restricted HNA. The shift from the A-type conformation found for the NMR solution structure recorded in pure water to the related A′-type structure obtained here under high-salt conditions (0.9 and 1.4 M Li_2SO_4) in the crystalline state obeys general principles of nucleic acid structure,[46] suggesting that the conformational rigidity in HNA compared to that in naturally occurring nucleic acids is less pronounced than previously assumed. This is of importance for enzymatic action on HNA, which commonly involves a structural change in helical conformation. However, HNA/RNA is only a poor substrate for RNAseH cleavage, though it is efficiently bound by the enzyme.[11] The large major groove width, which is similar in the NMR and X-ray crystal structures, probably determines the resistance of HNA/RNA against RNAseH, though all structural details of the minor groove and the conformational rigidity of HNA may have an additional influence.[12] By contrast, it has been shown that mutants of HIV-1 reverse transcriptase are able to successively elongate primers in a template-based manner with more than three hexitol nucleotides, demonstrating the feasibility of enzymatic action on HNA strands.[14]

Hydration has not previously been an issue in the NMR solution structure of HNA/RNA or in the crystal structure analysis of dsHNA, and a molecular dynamics investigation examined only differences in the hydration properties of HNA/RNA and HNA/DNA duplexes and compared their solvent accessible surfaces.[21] The analysis of the crystal structure presented here points for the first time to differences in hydration of the backbone phosphates in HNA and RNA strands. The slightly, but significantly altered geometry of the HNA backbone promotes a tighter bridging of adjacent phosphate O2P atoms by water molecules. This reinforced hydration has also been confirmed from two crystal forms of dsHNA oligonucleotides. The enhanced backbone hydration provides an additional explanation for the extraordinary stability of HNA/HNA and HNA/RNA hybrids as opposed to that of RNA/RNA duplexes, beyond the limited conformational rigidity of the hexitol group. For the future design of modified oligonucleotides, one should consequently consider not only the structural preorganization and nuclease resistance but also the optimization of hydration properties to enhance duplex stability.

The structural basis for enhanced spinelike hydration is slight alterations in the backbone geometry induced by the presence of a six-membered ring instead of the five-membered (deoxy)-ribose ring in naturally occurring nucleic acids. The reinforcing effect on hydration must be considered as a second contribution to the overall duplex stability by six-membered rings, in addition to the conformational preorganization imposed by them. Assuming that extreme duplex stability is hindering the highly dynamic remodeling of nucleic acids essential for biological information transfer, we determine that reinforced backbone hydration in nucleic acid analogues incorporating six-membered rings might be one reason for the observed evolutionary preference for ribose-derived nucleic acids.

Acknowledgment. We thank Claudia Alings for excellent technical assistance in crystal growth, and Philippe Carpentier for help with crystallographic data collection at BM30, ESRF Grenoble. These studies were supported by Deutsche Forschungsgemeinschaft (SA196/38,1-3) and by Fonds der Chemischen Industrie.

Supporting Information Available: Additional figures and tables. This material is available free of charge via the Internet at http://pubs.acs.org.

JA045843V

(46) Tolstorukov, M. Y.; Maleev, V. Y. *J. Biomol. Struct. Dyn.* **2000**, *17* (5), 913−920.